Iterative Joint PIC and 2D MMSE-FDE for Turbo-coded HARQ with SC-MIMO Multiplexing

Akinori Nakajima and Fumiyuki Adachi
Dept. of Electrical and Communications Engineering, Graduated school of Engineering,
Tohoku University, Sendai, Japan
nakajima@mobile.ecei.tohoku.ac.jp

Abstract— **Broadband wireless packet access will be the core technology of the next generation mobile communication systems. For very high-speed and high-quality packet transmissions, the joint use of multiple-input multiple-output (MIMO) multiplexing and hybrid ARQ (HARQ) is very effective. However, if single-carrier (SC) transmission is used, the transmission performance significantly degrades due to a large inter-symbol interference (ISI) resulting from a severe frequency-selective fading. Recently, we proposed a frequency-domain iterative parallel interference cancellation (PIC) for SC-MIMO multiplexing. For signal separation, 2 dimensional minimum mean square error (2D MMSE)-FDE is performed at first. Then, the joint PIC and 1D MMSE-FDE is repeated a sufficient number of times. However, the interference from other transmit antennas still remains at the outputs of PIC. Therefore, in this paper, we propose to use 2D MMSE-FDE instead of 1D MMSE-FDE in each iteration and investigate, by computer simulation, the achievable bit error rate (BER) and throughput performance of HARQ in a frequency-selective Rayleigh fading channel.**

Keywords- SC-MIMO multiplexing, 2D MMSE-FDE, Iterative PIC, RCPT-HARQ

I. INTRODUCTION

Recently, there have been tremendous demands for high-speed data transmissions higher than few tens of Mbps in mobile communications [1]. However, for such high-speed data transmissions, the channel consists of many resolvable paths with different time delays, resulting in a severely frequency-selective fading channel. The transmission performance of SC transmission significantly degrades due to a severe inter-symbol interference (ISI) [2]. Recently, it has been shown that the use of frequency-domain equalization (FDE) can significantly improve the SC transmission performance [3,4]. For wireless communication, however, the available bandwidth is limited, so highly spectrum-efficient transmission technique is required for the next generation mobile communication systems.

One of the promising techniques is the multiple-input multiple-output (MIMO) multiplexing [5], that uses multiple transmit and receive antennas. In MIMO multiplexing, a transmit data sequence is transformed into parallel sequences and each sequence is transmitted from a different transmit antenna at the same time with the same carrier frequency. Therefore, the total transmission data rate increases in proportion to the number of transmit antennas without requiring additional bandwidth. At a receiver, it is necessary to separate the signals transmitted from different antennas. A lot of research attention has been paid to find the signal separation methods, which provide a performance close to that of maximum likelihood detection (MLD) but with reduced complexity, like vertical-Bell laboratories layered space-time architecture (V-BLAST) [6], MLD using QR decomposition [7] and so on.

Recently, we proposed a frequency-domain iterative parallel interference cancellation (PIC) for SC-MIMO multiplexing in a frequency-selective fading channel [8]. For the separation of transmitted signals, at first, 2 dimensional minimum mean square error (2D MMSE)-FDE is used. Then, joint PIC and 1D MMSE-FDE is repeated a sufficient number of times. However, 1D MMSE-FDE can only suppress the ISI, but the interference from other antennas still remains at the outputs of PIC. Therefore, in this paper, 2D MMSE-FDE is used instead of 1D MMSE-FDE in each iteration.

Packet access will be the core technology of the next generation mobile communication systems. Very high-speed and high-quality packet transmissions in a limited bandwidth can be achieved by the joint use of MIMO multiplexing and hybrid automatic repeat request (HARQ). However, to the best of authors' knowledge, the throughput performance of HARQ with SC-MIMO multiplexing has not yet been fully investigated. In this paper, we evaluate, by computer simulation, the bit error rate (BER) performance of SC-MIMO multiplexing using iterative joint PIC and 2D MMSE-FDE, which considers the interference from other antennas in a frequency-selective Rayleigh fading channel. We then evaluate the throughput performance of rate compatible punctured turbo coded (RCPT) HARQ [9]. The remainder of this paper is organized as follows. Section II and III describe the SC-MIMO multiplexing with the frequency-domain iterative PIC and RCPT-HARQ, respectively. Section IV presents the computer simulation results of the BER and throughput performances. Section V concludes the paper.

II. FREQUENCY-DOMAIN ITERATIVE PIC USING 2D MMSE-FDE FOR SC-MIMO MULTIPLEXING

A. *Transmitted and received signal*

Fig.1 shows the transmitter/receiver structure of SC-(N_t,N_r)MIMO multiplexing using frequency-domain iterative PIC. N_t transmit antennas and N_r receive antennas are used. At the transmitter, turbo coding is performed on the CRC coded binary information sequence, and the transmitted sequences obtained by puncturing the turbo coded sequence are stored in the buffer. In this paper, RCPT type II HARQ [10] is considered.

After bit-interleaving and data-modulation, for MIMO multiplexing, the data-modulated symbol sequence is serial-to-parallel (S/P) converted to N_t parallel sequences, each to be transmitted from a different transmit antenna. In this paper, QPSK data-modulation is considered. Each QPSK modulated symbol sequence is divided into a sequence of blocks of N_c symbols each. The data symbol, transmitted from the n_tth antenna at time t, is denoted by $s_{n_t}(t)$, where t=0~N_c-1. The last N_g symbols in each block are copied and inserted as a cyclic prefix into the guard interval (GI), placed at the beginning of each block, to form a frame with N_g+N_c symbols.

N_t transmitted blocks are transmitted simultaneously in parallel from N_t transmit antennas using the same carrier frequency. At the receiver, a superposition of N_t transmitted signals is received by N_r antennas via a frequency-selective fading channel. The channel is assumed to be a symbol-spaced L-path frequency-selective fading channel, each discrete propagation path being subjected to independent fading. After the removal of the GI from the received signal, N_c-point fast Fourier transform (FFT) is applied to decompose the GI-removed received signal $r_{n_r}(t)$, t=0~N_c-1, into N_c frequency components. The kth frequency component $R_{n_r}(k)$ of the received signal on the n_rth antenna is expressed as

$$R_{n_r}(k)=\sqrt{2S}\sum_{n_t=0}^{N_t-1}H_{n_r,n_t}(k)S_{n_t}(k)+\Pi_{n_r}(k)\text{ , (1)}$$

where S is the received signal power per antenna, $H_{n_r,n_t}(k)$ is the complex channel gain between the n_tth transmit antenna and the n_rth receive antenna, $S_{n_t}(k)$ is the transmitted signal component, and $\Pi_{n_r}(k)$ is the noise component. They are given by

$$\begin{cases}H_{n_r,n_t}(k)=\sum_{l=0}^{L-1}h_{n_r,n_t,l}\exp(-j2\pi\tau_l\,k/N_c)\\ S_{n_t}(k)=\sum_{t=0}^{N_c-1}s_{n_t}(t)\exp(-j2\pi t\,k/N_c)\\ \Pi_{n_r}(k)=\sum_{t=0}^{N_c-1}n_{n_r}(t)\exp(-j2\pi t\,k/N_c)\end{cases}\text{ , (2)}$$

where $h_{n_r,n_t,l}$ denotes the lth path gain between the n_rth receive antenna and n_tth transmit antenna, $n_{n_r}(t)$ is a zero-mean complex Gaussian process having a variance $2N_0/T_s$ with N_0 being the one-sided power spectrum density of additive white Gaussian noise (AWGN) and T_s being the symbol length.

B. Joint PIC and 2D MMSE-FDE

At the initial stage (i=0), two dimensional (2D) FDE based on MMSE criterion is applied to suppress the ISI due to frequency-selective fading and the interference from other transmit antennas. However, the initial 2D MMSE-FDE can not sufficiently suppress the interference. Hence, we perform joint 2D MMSE-FDE and frequency-domain PIC in an iterative fashion. Fig.2 shows the frequency-domain iterative PIC.

1) 2D MMSE-FDE

a) i=0

The n_tth transmitted signal component $\widetilde{R}^{(i)}_{n_t}(k)$ at the kth frequency after 2D MMSE-FDE in the i=0th iteration is given as

$$\widetilde{R}^{(0)}_{n_t}(k)=\mathbf{W}^{(0)}_{n_t}(k)\mathbf{R}(k)\text{ , (3)}$$

where $\mathbf{R}(k)=[R_0(k),\quad ,R_{N_r-1}(k)]^T$ is the N_r-by-1 received signal vector at the kth frequency. $\mathbf{W}^{(0)}_{n_t}(k)$ is the 1-by-N_r 2D MMSE weight vector for the n_tth transmitted signal and can be derived from [2] as

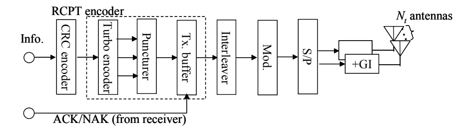

(a) Transmitter

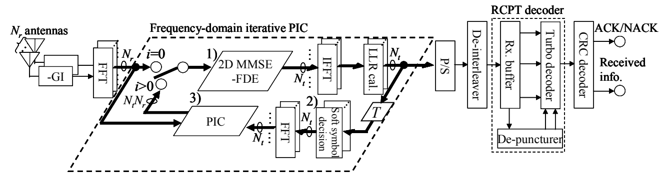

(b) Receiver

Figure 1 Transmitter/receiver structure.

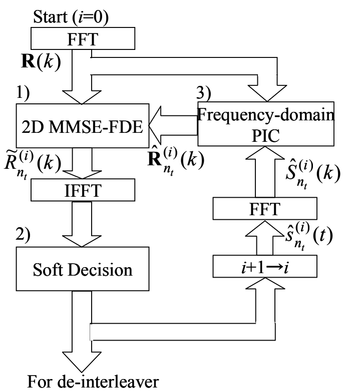

Figure 2 Frequency-domain iterative joint PIC and 2D MMSE-FDE.

$$\mathbf{W}^{(0)}_{n_t}(k)=\mathbf{H}^H_{n_t}(k)[\mathbf{H}(k)\mathbf{H}^H(k)+(E_s/N_0)^{-1}\mathbf{I}]^{-1}\text{ , (4)}$$

where $\mathbf{H}(k)$ is the N_r-by-N_t complex channel gain matrix whose component of the n_rth row and n_tth column is $H_{n_r,n_t}(k)$, $\mathbf{H}_{n_t}(k)$ is the n_tth column vector of $\mathbf{H}(k)$, E_s/N_0 (=ST_s/N_0) represents the average received symbol energy-to-AWGN power spectrum density ratio, $\mathbf{I}$ is the N_r-by-N_r identity matrix, and $(.)^H$ is the Hermit transpose operation.

b) i ≥ 1

Since the interference from the other transmit antennas can be only partially cancelled by performing PIC, the interference still remains at the outputs of PIC. Then, 2D MMSE-FDE is performed to obtain the n_tth transmitted signal component $\widetilde{R}^{(i)}_{n_t}(k)$ at kth frequency in the ith iteration as

$$\widetilde{R}^{(i)}_{n_t}(k)=\mathbf{W}^{(i)}_{n_t}(k)\hat{\mathbf{R}}_{n_t}(k)\text{ , (5)}$$

where $\hat{\mathbf{R}}^{(i)}_{n_t}(k)=[\hat{R}^{(i)}_{n_t,0}(k),\quad ,\hat{R}^{(i)}_{n_t,N_r-1}(k)]$ is the kth frequency signal component vector, after PIC in the ith iteration, associated with the signal transmitted from the n_tth antenna. $\mathbf{W}^{(i)}_{n_t}(k)$ is the 1-by-N_r 2D MMSE weight vector for the n_tth transmitted signal and is given by

$$\mathbf{W}^{(i)}_{n_t}(k)=\mathbf{H}^H_{n_t}(k)[\mathbf{H}(k)\mathbf{G}^{(i)}_{n_t}\mathbf{H}^H(k)+(E_s/N_0)^{-1}\mathbf{I}_{N_r}]^{-1}\text{ , (6)}$$

where $\mathbf{G}_{n_t}^{(i)} = diag[g_{n_t,0}^{(i)}, \quad ,g_{n_t,N_t-1}^{(i)}]$ is the interference coefficient matrix and $g_{n_t,n_t'}^{(i)}$ reflects the residual interference from the n_t'th antenna to the n_tth antenna. $g_{n_t,n_t'}^{(i)}$ is given by

$$g_{n_t,n_t'}^{(i)} = \begin{cases} 1-(1/N_c)\sum_{t=0}^{N_c-1}|\hat{s}_{n_t'}^{(i)}(t)|^2 & if\ n_t' \neq n_t \\ 1 & otherwise \end{cases}, \quad (7)$$

where $\hat{s}_{n_t'}^{(i)}(t)$ is the replica of symbol block transmitted from the n_t'th antenna to be used in the ith iteration.

On the other hand, when 1D MMSE-FDE is used, 1D MMSE-FDE operation is the same as Eq. (5), but $\mathbf{W}_{n_t}^{(i)}(k)$ is obtained by setting $g_{n_t,n_t'}^{(i)} = 0 \ (n_t' \neq n_t)$ (i.e., the interference from other antennas is neglected).

2) Soft symbol replica generation

The received symbol block $\tilde{s}_{n_t}^{(i-1)}(t)$, t=0~N_c-1, is obtained by performing N_c-point IFFT on $\{\tilde{R}_{n_t}^{(i-1)}(k)$; k=0~N_c-1$\}$ after carrying out 2D MMSE-FDE in the (i-1) th iteration. Then, the log likelihood ratio (LLR), $\lambda_{n_t,b}^{(i-1)}(t)$, of the bth bit (b=0,1) in the tth symbol transmitted from the n_t transmit antenna, is computed by using $\tilde{s}_{n_t}^{(i-1)}(t)$ [11]. Then, the replicas of N_t symbol blocks, $\{\hat{s}_{n_t}^{(i)}(t)$; n_t=0~ N_t-1$\}$ to be used in the ith iteration, are generated by using $\{\lambda_{n_t,b}^{(i-1)}(t)$; b=0,1$\}$ [8] as

$$\hat{s}_{n_t}^{(i)}(t) = \left(1/\sqrt{2}\right)\left\{\tanh(\beta\lambda_{n_t,0}^{(i-1)}(t)/2) + j\tanh(\beta\lambda_{n_t,1}^{(i-1)}(t)/2)\right\}, \quad (8)$$

where β is a parameter that controls the extent to which the soft decision contributes to the replica generation.

3) PIC operation

N_c-point FFT is performed on $\{\hat{s}_{n_t}^{(i)}(t)$; n_t=0~N_t-1$\}$ to obtain the frequency-domain signal replica $\{\hat{S}_{n_t}^{(i)}(k)$; k=0~N_c-1$\}$. For PIC operation, the frequency-domain interference replica $\sqrt{2S}\sum_{n_t'=0, \neq n_t}^{N_t-1} H_{n_r,n_t'}(k)\hat{S}_{n_t'}^{(i)}(k)$ is generated and subtracted from the signal component $R_{n_r}(k)$ to extract the kth frequency component $\hat{R}_{n_r,n_t}^{(i)}(k)$ of the signal transmitted from the n_tth antenna. The PIC operation to extract $\hat{R}_{n_r,n_t}^{(i)}(k)$ is expressed as

$$\hat{R}_{n_r,n_t}^{(i)}(k) = R_{n_r}(k) - \sqrt{2S}\sum_{\substack{n_t'=0 \\ \neq n_t}}^{N_t-1} H_{n_r,n_t'}(k)\hat{S}_{n_t'}^{(i)}(k). \quad (9)$$

The above processes 1)~3) are repeated a sufficient number of times. Then, deinterleaving and RCPT decoding are performed. In the RCPT decoder, depuncturing, turbo decoding, and error detection are performed. The result of error detection is transmitted to the transmitter as ACK/NACK.

III. RCPT TYPE II HARQ

In this paper, RCPT type II HARQ [10] is applied. Turbo encoder of coding rate R=1/3 is considered. The turbo encoder outputs the systematic bit (information bit) sequence and two parity bit sequences, each has a length of K bits. In this paper, three type II schemes are considered, represented by S-Px and x different sequences of length 2K/x are obtained. In what follows, for simplicity, S-P2 is explained. The schematic diagrams are shown in Fig.3. The 1st transmit packet consists of the systematic bit sequence only and the 2nd and 3rd are taken from two punctured parity bit sequences. The following puncturing matrices are used for the 1st, 2nd and 3rd transmissions [10]:

$$\begin{bmatrix} 1 & 1 \\ 0 & 0 \\ 0 & 0 \end{bmatrix}, \begin{bmatrix} 0 & 0 \\ 1 & 0 \\ 0 & 1 \end{bmatrix}, \begin{bmatrix} 0 & 0 \\ 0 & 1 \\ 1 & 0 \end{bmatrix}.$$

Fig.4 shows HARQ protocols. At the transmitter, the first packet, consisting of systematic bit sequence only, is transmitted. At the receiver, error detection is performed. If any error is detected in the received packet, an NACK is transmitted to the transmitter. Then, the second packet is transmitted. At the receiver, depuncturing is performed, followed by turbo decoding. In this case, turbo coding corresponds to R=1/2. After turbo decoding, the error detection is performed. If any error is detected, the receiver transmits the NACK again. At the transmitter, another punctured parity bit sequence is transmitted. At the receiver side, the second and third received packets are transformed into two parity bit sequences by depuncturing and then, R=1/3 turbo decoding is carried out again.

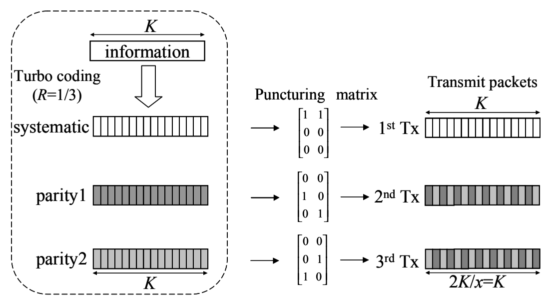

Figure 3 Transmit packet generation for RCPT type II HARQ S-P2.

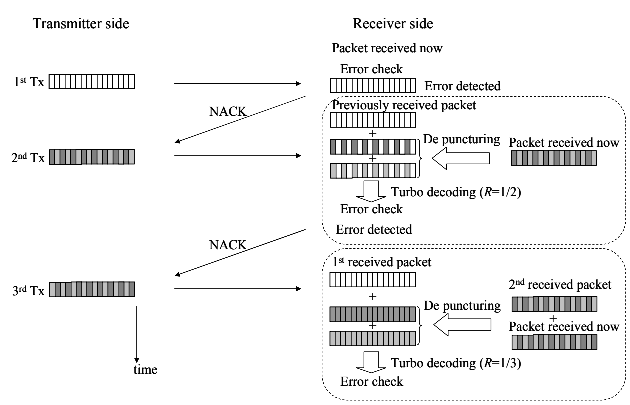

Figure 4 HARQ protocol.

Table 1. Simulation conditions.

Data Modulation		QPSK
Number of Tx, Rx Antennas		N_t=N_r=4
Number of FFT points		N_c=256
GI		N_g=32
Channel	Frequency-selective block Rayleigh fading	
	L=16-path exponential power delay profile	
	Decay factor α=0, 6dB	
Channel estimation		Ideal

IV. COMPUTER SIMULATION

The simulation parameters are given in Table 1. We assume an information bit sequence of K=2048 bits. Coding rate R=1/3 turbo encoder, consisting of two (13,15) recursive systematic convolutional (RSC) encoders, is employed. We assume that N_r-by-N_t channels are independent and identically distributed frequency-selective block Rayleigh fading channels, each channel has a symbol-spaced exponentially decaying L=16-path power delay profile with decay factor α. Ideal channel estimation is assumed. Each transmit symbol block is composed of N_c=256 symbols and the GI length is N_g=32 symbols.

The uncoded BER performance of SC-(4,4)MIMO multiplexing is plotted in Fig.5 as a function of the average received energy per bit-to-noise power spectrum density ratio E_b/N_0 per receive antenna. As the number of iterations increases, the BER performance improves but the additional improvement becomes smaller. When α=0dB (strong frequency-selectivity), i=3 iterations is sufficient for both 1D and 2D MMSE-FDE. 2D MMSE-FDE provides only slightly better BER performance than 1D MMSE-FDE. However, when α=6dB (weak selectivity), 2D MMSE-FDE provides much better performance than 1D MMSE-FDE. The required E_b/N_0 is smaller by about 3dB with 2D MMSE-FDE than with 1D MMSE-FDE. For comparison, the result of the perfect PIC case (i.e., the interference from other antennas is perfectly cancelled) is also plotted. The E_b/N_0 degradation from the perfect PIC case is about 0.4dB and 2.4dB, when α=0 and 6dB, respectively.

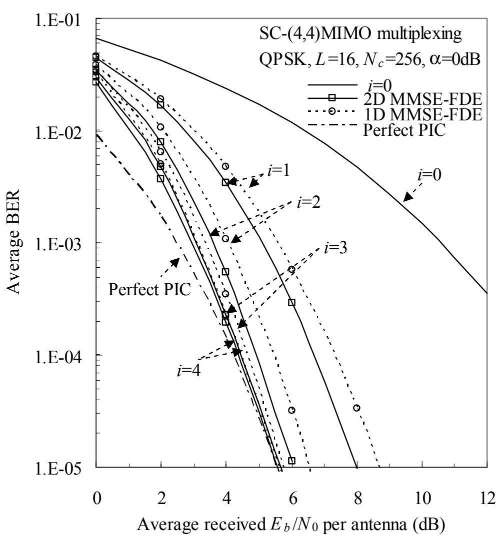

(a) α=0dB

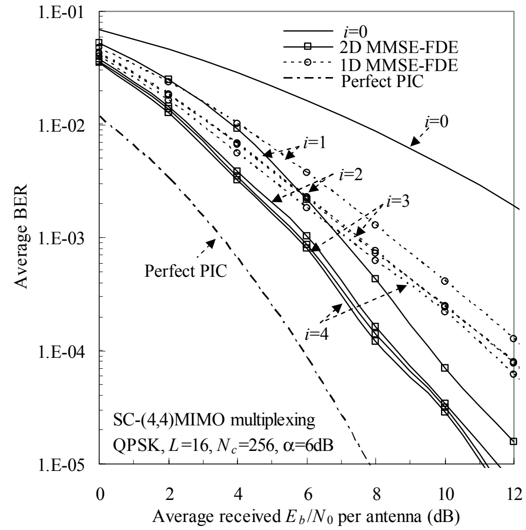

(b) α=6dB

Figure 5 Uncoded BER performance.

The throughput performance of RCPT type II HARQ S-P2 for SC-(4,4)MIMO multiplexing is plotted in Fig.6 as a function of the average received energy per symbol-to-noise power spectrum density ratio E_s/N_0 per receive antenna. The throughput can be significantly improved by the use of iterative joint PIC and 2D MMSE-FDE. The required E_s/N_0 for the throughput of 6.5 bps/Hz can be reduced by about 7~9dB by the use of i=3 iterations. As is expected from Fig.5, 2D MMSE-FDE and 1D MMSE-FDE provide similar throughput performance when α=0dB (strong selectivity); however, the former provides much higher throughput performance when α=6dB (weak selectivity). The required E_s/N_0 for the throughput of 6.5 bps/Hz is about 2.7 dB smaller with 2D MMSE-FDE than with 1D MMSE-FDE.

Fig. 7 shows the throughput of type II HARQ with S-Px. When α=0dB, the throughput performance with 2D MMSE-FDE is slightly better than that with 1D MMSE-FDE. However, when α=6dB, the frequency diversity gain is smaller and hence the probability of successful first transmission is lower than when α=0dB. Therefore, more retransmissions are required, resulting in the reduced throughput. 2D MMSE-FDE provides much higher throughput than 1D MMSE-FDE. Irrespective of the channel selectivity (α=0 and 6dB), S-P8 is the best between the three schemes. This is because in S-P8 scheme, the transmission of unnecessary redundant bits is avoided so that the number of bits, transmitted in the second transmission onwards, is less. However, S-P8 has a larger delay time since it requires more retransmissions.

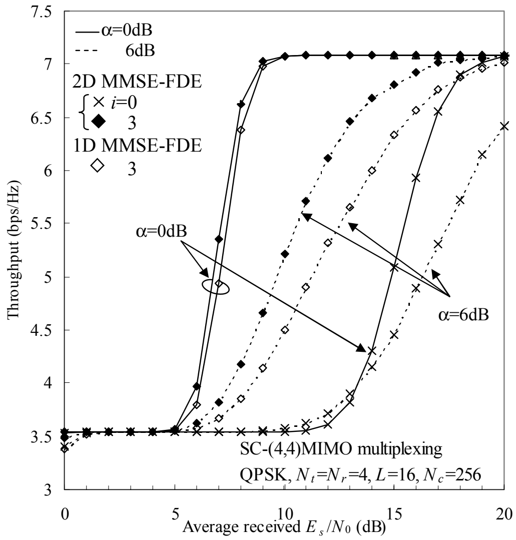

Figure 6 Throughput performance of S-P2.

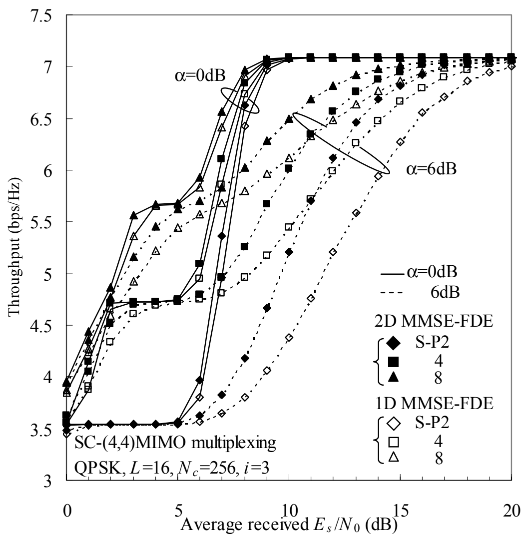

Figure 7 Throughput comparison of S-P2, 4 and 8.

V. CONCLUSIONS

In this paper, we proposed iterative joint PIC and 2D MMSE-FDE for SC-MIMO multiplexing. The MMSE weight for 2D MMSE-FDE was derived taking into account the interference from other antennas after performing PIC. We evaluated, by computer simulation, the BER performance and the turbo-coded HARQ throughput performance in a frequency-selective Rayleigh fading channel. For the strong channel frequency-selectivity case, the use of 2D MMSE-FDE provides slightly better BER and throughput performances than 1D MMSE-FDE; however, it provides much better performances in the case of weak channel frequency-selectivity.

REFERENCES

[1] F. Adachi, "Wireless past and future-evolving mobile communications systems," IEICE Trans. Fundamentals, vol.E83-A, No.1, pp.55-60, Jan. 2001.

[2] John G. Proakis, *Digital Communications*, 4th edition, McGraw-Hill, 2001.

[3] D. Falconer, et al., "Frequency domain equalization for single-carrier broadband wireless systems," IEEE Commun. Mag., vol.40, pp.58-66, April 2002.

[4] K. Takeda, et al., "Joint use of frequency-domain equalization and transmit/receive antenna diversity for single-carrier transmissions," IEICE Trans. Commun., vol. E87-B, no.7, pp.1946-1953, July 2004.

[5] G. J. Foschini, et al., "On of wireless communications in a fading environment when using multiple antennas," Wireless Personal Communi., Vol.6, No. 3, pp. 311-335, Mar. 1998.

[6] P. W. Wolniansky, et al., "V-BLAST: an architecture for realizing very high data rates over the rich-scattering wireless channel," Proc. ISSSE, pp.295-300, Italy Sept. 1998.

[7] H. Kawai, et al., "Likelihood function for QRM-MLD suitable for soft-decision turbo decoding and its performance for OFCDM MIMO multiplexing in multipath fading channel," IEICE Trans. Commun., vol E88-B, No.1, pp.47-57, Jan. 2005.

[8] A. Nakajima, et al., "Throughput of turbo coded hybrid ARQ using single-carrier MIMO multiplexing," Proc. IEEE VTC2005-Spring, Stockholm, Sweden, April 2005.

[9] J. Hagenauer, et al., "Rate-compatible punctured convolutional codes (RCPC codes) and their application," IEEE Trans. Commun., vol. 36, no. 4, pp.389-400, April 1988.

[10] D. Garg, et al., "Rate compatible punctured turbo-coded hybrid ARQ for OFDM in a frequency selective fading channel," Proc. IEEE VTC2003-Spring, pp.2725-2729, Jeju, Korea, April 2003.

[11] A. Stefanov, et al., "Turbo coded modulation for wireless communications with antenna diversity," J. Commun. Netw., vol. 2, no. 4, pp. 356-360, Dec. 2000.